2002

Dynamics of a Granular Particle on a Rough Surface With a Staircase Profile

J. J. P. Veerman
Portland State University, veerman@pdx.edu

F. V. Cunha Jr.
Universidade Federal de Pernambuco

G. L. Vasconcelos
Universidade Federal de Pernambuco

Dynamics of a granular particle on a rough surface with a staircase profile

J. J. P. Veerman

Mathematical Sciences, Portland State University, Portland, OR 97207, USA.

F. V. Cunha, Jr., G. L. Vasconcelos

Laboratório de Física Teórica e Computacional, Departamento de Física, Universidade Federal de Pernambuco, 50670-901, Recife, Brazil.

Abstract

A simple model is presented for the motion of a grain down a rough inclined surface with a staircase profile. The model is an extension of an earlier model of ours where we now allow for bouncing, i.e., we consider a non-vanishing normal coefficient of restitution. It is shown that in parameter space there are three regions of interest: i) a region of smaller inclinations where the orbits are always bounded (and we argue that the particle always stops); ii) a transition region where halting, periodic and unbounded orbits co-exist; and iii) a region of large inclinations where no halting orbit exists (and we conjecture that the motion is always unbounded). Fixed points are also found at precisely the inclination separating regions i) and ii).

Key words: Grain dynamics, Granular flow, Friction, Nonlinear dynamics
PACS: 45.70.-n
PACS: 83.70.-f
PACS: 45.50.-j

1 Introduction

The gravity-driven flow of granular materials is a topic of considerable interest because of its obvious practical importance as well as for scientific reasons. Here the interplay between the driving force (gravity) and dissipation (inelastic grain collisions) can lead to a range of complex dynamical behaviors, such as intermittent flow (i.e., avalanches), and continuous steady and unsteady flows [1,2]. A complete understanding of the grain dynamics during such flows remains a challenge [3]. Thus, the study of simple models for grain dynamics

is of great interest since they might provide useful insights into the actual dynamics of granular flows. In this context, the motion of a single grain on a rough inclined surface has recently been studied both experimentally [4] and theoretically [5–9].

Motivated by some of these studies, we have recently introduced [10,11] a class of models for the gravity-driven motion of a single grain down a rough inclined surface, where some simplifying assumptions were made: (i) the rough surface was supposed to have a simple 'staircase' profile; (ii) the grain was treated as a point particle; and (iii) a simple restitution law was adopted, namely, $v_t' = C(v_t, v_n)$ and $v_n' = 0$, where v_t and v_n are the velocity components tangential and normal to the collision plane, with the prime denoting post-collisional velocities, and $C(x, y)$ is a homogeneous function of degree 1 [11]. The no-bouncing condition ($v_n' = 0$) was adopted so that the dynamics of the model could be reduced to a one-dimensional map. (To see this, note that upon colliding with a step the particle slides to the end of this step, at which point it takes off, and so on; hence we only need to keep track of the tangential velocity at takeoff.) First we analyzed the simpler case in which $C(v_t, v_n) = e_t v_t$, where e_t is the tangential coefficient of restitution. Here it was found that, as the surface inclination increases, there is a sharp transition (independent of initial conditions) from a regime of bounded velocities to a an accelerated regime. In the bounded regime itself, there is a transition from steady motion (corresponding to stable fixed points) to unsteady (chaotic) behavior [10]. Another important result was the fact shown in Ref. [11] that the qualitative nature of the phase diagram of the model is preserved for any physically reasonable choice of the function $C(v_t, v_n)$.

In the present paper, we consider an extension of our previous model where we now include the case of a nonzero normal restitution coefficient e_n. More specifically, here we adopt the following collision rule:

$$v_t' = e_t v_t, \tag{1}$$
$$v_n' = -e_n v_n, \tag{2}$$

where both e_t and e_n take values in the interval $[0, 1)$. Regarding these collision conditions, it should be pointed out that in view of the discussion at the end of the preceding paragraph, the choice (1) may not be as restrictive as it might seem at first. As for condition (2), experiments on binary collisions between spheres have shown that the normal restitution law is well described by a single normal coefficient of restitution [12]. As it will be seen below, our model is now described by a three-dimensional map which displays a much richer dynamics. One striking difference from our original model [10] is that in the present model the transition from bounded to unbounded orbits is no longer sharp: there is an intermediate region where both bounded and unbounded orbits coexist. Moreover, in this transition region we also find infinitely many

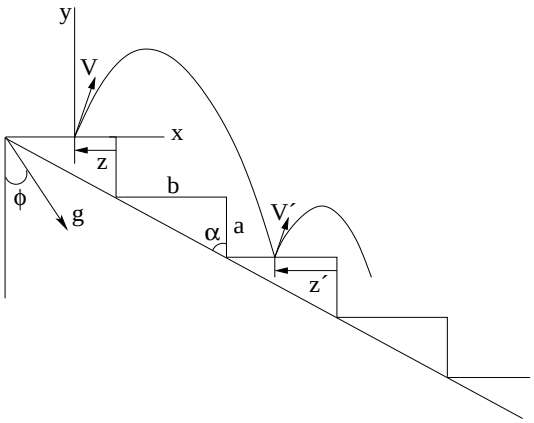

Fig. 1. Model for a single particle moving under gravity on an rough inclined surface.

periodic orbits. We conjecture (and give evidences) that below this transition region, the particle always comes to a halt, whereas above it the particle always accelerates.

It is interesting to note that certain dynamical features in the original model [10], most prominently the existence of unstable fixed points, are due to the condition of no-bouncing and subsequent sliding. In the bouncing model discussed in the present paper only *stable* fixed points and periodic orbits can occur. (In [13] we have presented a preliminary analysis of a hybrid model that contains aspects of both models, where we allow sliding after the particle stops bouncing.)

The paper is organized as follows. In Sec. 2 we describe our model. In Sec. 3 we give conditions for which unbounded orbits can exist, whereas in Sec. 4 we discuss when halting orbits occur. The issue of existence of fixed points and periodic orbits is then tackled in Secs. 5 and 6, respectively. Sec. 7 contains additional discussion about our findings as well as our conclusions. We anticipate here, in particular, that the main results of the paper are summarized in the 'phase diagram' shown in this last section in Fig. 2.

2 The Model

In our model, which is shown in Fig. 1, the rough surface is considered to have a simple staircase shape whose steps have height a and length b [10]. For convenience, we choose a system of coordinates such that the step plateaus are aligned with the x axis and the direction of the acceleration of gravity $\mathbf{g}$ makes an angle ϕ with the y axis. A particle is then launched on the top of the 'staircase' with a given initial velocity, so that its subsequent motion will consist of a sequence of ballistic flights and collisions, as illustrated in Fig. 1.

Suppose that our particle starts a given flight with velocity (u, v) and that the launching point is taken as the origin. The particle will undergo a ballistic flight until it collides with another plateau located a certain number n of steps below the departure step—the integer n will thus be referred to as the *jump number* for the flight. If the time of flight from departure to landing is denoted by t, then the velocity (u_c, v_c) at collision and the corresponding collision point (x_c, y_c) are determined by

$$\begin{aligned} u_c &= u + gst, \\ v_c &= v - gct, \\ x_c &= ut + \tfrac{1}{2}gst^2, \\ y_c &= vt - \tfrac{1}{2}gct^2 \;\; = -na. \end{aligned} \tag{3}$$

Here for ease of notation we have defined the parameters $s \equiv \sin\phi$ and $c \equiv \cos\phi$. Notice that u_c is positive whereas v_c is negative. The last equation can be solved for the flight time t, which in turn can be used to yield the particle velocity and position at collision. Before doing this, however, it is best to simplify the equations above by defining new variables.

First, let z denote the distance from the starting point of the current flight to the edge of the horizontal ramp where the flight started; see Fig. 1. Then the position z' at the beginning of next flight will be

$$z' = z + nb - x_c \quad . \tag{4}$$

Note that we always have

$$0 \le z < b \quad . \tag{5}$$

In fact, this latter requirement determines the value of the discrete variable n, that is, n is the smallest integer such that the condition (5) holds for z'.

Next, we define dimensionless variables:

$$\begin{aligned} X &= \frac{x}{b}, & Y &= \frac{y}{a}, & Z &= \frac{z}{b}, \\ U &= \frac{c}{s}\frac{u}{\sqrt{2gca}}, & V &= \frac{v}{\sqrt{2gca}}, & T &= \sqrt{\frac{gc}{2a}}\, t\,. \end{aligned} \tag{6}$$

Subsequently we drop the capital notation with the understanding that we shall be working solely with dimensionless variables. In these new variables,

the equations given in (3) become

$$\begin{aligned} u_c &= u + t, \\ v_c &= v - t, \\ x_c &= 2\kappa u t + \kappa t^2, \\ y_c &= 2vt - t^2 = -n, \end{aligned} \tag{7}$$

where we have introduced a new parameter κ defined by

$$\kappa \equiv \frac{\tan\phi}{\tan\alpha} = \frac{s}{c}\frac{a}{b}.$$

Note also that (4) simplifies to

$$z' = z + n - x_c \quad , \tag{8}$$

with $0 \leq z < 1$. The last equation in (7) can easily be solved for the re-scaled time of flight:

$$t = v + (v^2 + n)^{1/2}. \tag{9}$$

Inserting (9) into the first three equations in (7) yields the velocity (u_c, v_c) and the position x_c at collision as a function of u, v and z. Now, if we denote by (u', v') the particle velocity immediately after the collision, then according to the collision law given in (1) and (2) we have $u' = e_t u_c$ and $v' = -e_n v_c$, whereas the corresponding coordinate z' is obtained by plugging x_c into (8). Performing this calculation, one obtains that the dynamics of the model is described by the following map

$$F : (u, v, z) \to (u', v', z'), \tag{10}$$

where

$$\begin{aligned} u' &= e_t \left(u + v + \sqrt{v^2 + n}\right), \\ v' &= e_n \sqrt{v^2 + n}\,, \\ z' &= z + n(1 - \kappa) - 2\kappa(u + v)\left(v + \sqrt{v^2 + n}\right). \end{aligned} \tag{11}$$

We note here for later use that the equation above for the variable z can be

conveniently written as

$$z' = z + n - \kappa \left(\frac{u'^2}{e_t^2} - u^2 \right). \tag{12}$$

As already mentioned, the jump number n appearing in (11) is determined by the requirements that n be the smallest non-negative integer such that $z' \geq 0$. Here there are two cases two consider: either (i) the particle lands on the very same step where the flight started, in which case $n = 0$, or (ii) it will jump at least one step so that $n > 0$. First consider case (i). Solving the equation $z'(n = 0) \geq 0$ gives the following condition:

$$\text{if} \quad z \geq 4\kappa v(u + v) \quad \text{then} \quad n = 0. \tag{13}$$

Otherwise, we have $n > 0$. In this case, in order to determine the exact value of n we first note that the equation for z' in (11) can be written as a quadratic expression in $\sqrt{v^2 + n}$. A careful investigation of the roots of this equation shows that if the inequality in (13) fails, then the quadratic equation has two distinct roots, with precisely one of which being greater than v. This means that n is the smallest positive integer such that $\sqrt{v^2 + n}$ is greater than this largest root. More specifically, one obtains that whenever inequality (13) fails the jump number n is determined by the condition

$$\sqrt{v^2 + n} \geq \frac{\kappa(u + v) + \sqrt{(\kappa u + v)^2 - (1 - \kappa)z}}{1 - \kappa} > \sqrt{v^2 + n - 1}. \tag{14}$$

Solving this equation for n then yields

$$n = \left\lceil \frac{2\kappa(u + v)}{(1 - \kappa)^2} \left[\kappa u + v + \sqrt{(\kappa u + v)^2 - (1 - \kappa)z} \right] - \frac{z}{1 - \kappa} \right\rceil,$$

where $\lceil x \rceil$ denotes the ceiling function (i.e., the smallest integer greater than x).

3 Bounded *vs.* Unbounded Orbits

Here we investigate the conditions under which the map F can have *unbounded orbits*, i.e., orbits for which the velocity grows indefinitely, or else when all orbits remain unbounded. Our main result is stated below.

Theorem 1 *The map F defined in (10) and (11) admits unbounded orbits if $\kappa > \kappa_\infty$, and all orbits are bounded if $\kappa < \kappa_\infty$, where*

$$\kappa_\infty = \frac{(1-e_t)(1-e_n)}{(1+e_t)(1+e_n)}. \tag{15}$$

Proof. We first note that for given κ, e_t, and e_n, it is clear that if at least one of u or v is very large then under iteration of map (11) the new u', v', and n' will be large. Let us then define the following quantity

$$\gamma \equiv \sqrt{v^2+n} - \frac{2\kappa u + (1+\kappa)v}{1-\kappa}. \tag{16}$$

Using this definition, we can rewrite the equations for u' and v' given in (11) as

$$u' = \frac{e_t}{1-\kappa}\left[(1+\kappa)u + 2v\right] + e_t\gamma, \tag{17}$$

$$v' = \frac{e_n}{1-\kappa}\left[2\kappa u + (1+\kappa)v\right] + e_n\gamma. \tag{18}$$

Now, when u and v are sufficiently large, it is shown in the Appendix that γ becomes arbitrarily small and hence (u', v') will grow if and only if the linearized model (i.e., with $\gamma = 0$) predicts growth. As is well known, a linear map will predict growth if its derivative matrix has at least one eigenvalue (Floquet multiplier) greater than unity. One can easily verify that the characteristic polynomial of the derivative matrix of the linear part of the map is

$$p(\lambda) = \lambda^2 - (e_n + e_t)\frac{(1+\kappa)}{(1-\kappa)}\lambda + e_t e_n.$$

One can now readily check that this polynomial has a root greater than 1 if and only if $\kappa > \kappa_\infty$. □

We remark that the case $\kappa = \kappa_\infty$ is left undecided by theorem above. We will see shortly, however, that in this case the map F has fixed points with any given jump number n and that the dynamics will always be attracted to one of such fixed points, so that for $\kappa = \kappa_\infty$ the orbits stay bounded as well.

A second noteworthy remark is that a model recently studied by Bideau and Valance [8] is a particular case of our map above with $\gamma = 0$ and $e_t = e_n = e$. If we neglect the physical dimension of the steps in our map (11), then their

continuous map follows. The particle in this case always lands on the line $y = -x$. Thus, in our notation, their model replaces the last equation of (7) by

$$y = 2vt - t^2 = -x \quad . \tag{19}$$

Solving for the re-scaled time of flight t yields

$$t = \frac{2(u+v)}{1-\kappa} \quad .$$

Substituting t back into (7) gives us precisely the linear part of equations (17) and (18).

4 Halting Orbits

One particularly interesting class of bounded orbits in our model is what we term *halting orbits*, where the particle will bounce infinitely many times on the same step (i.e., $n = 0$), with ever smaller velocity, until coming eventually to a stop. By a *non-trivial halting orbit* we mean an orbit during which the particle jumps at least once with $n > 0$ before coming to a halt. Our goal in this section is to establish the conditions for the existence of such halting orbits.

We begin by considering the motion of our particle on a *single tilted ramp*, by which we mean a step of arbitrarily large size (i.e., $b \to \infty$ in Fig. 1). Let us then define the *stopping distance* d as the distance (measured along the ramp) from the point of the first takeoff to the point where the particle finally stops.

Lemma 2 *Let u and v be the velocity components at the beginning of the first flight on a single ramp, then the stopping distance d is given by*

$$d = 4\kappa \frac{(1+e_t e_n)v^2 + (1-e_n^2)uv}{(1-e_t e_n)(1-e_n^2)}. \tag{20}$$

Proof. To obtain the equation of motion on a single ramp, set $n = 0$ in (11):

$$u' = e_t(u+2v), \tag{21}$$
$$v' = e_n v, \tag{22}$$
$$z' = z - 4\kappa v(v+u). \tag{23}$$

Note that for the velocity we have a linear map. Thus, if we introduce matrix notation and write the initial velocity vector as

$$V = \begin{pmatrix} u \\ v \end{pmatrix}, \tag{24}$$

then the next iterate V' can be written as $V' = AV$, where the matrix A is

$$A = \begin{pmatrix} e_t & 2e_t \\ 0 & e_n \end{pmatrix}. \tag{25}$$

More generally, the velocity V_k after k iterations will be $V_k = A^k V$, with

$$A^k = \begin{pmatrix} e_t^k & 2\sum_{i=1}^{k} e_t^i e_n^{k-i} \\ 0 & e_n^k \end{pmatrix}, \tag{26}$$

Note also that the distance (measured along the ramp) advanced by the particle over one iteration can be written with the usual *scalar product notation*:

$$z - z' = (V, BV), \tag{27}$$

where the matrix B is given by

$$B = 2\kappa \begin{pmatrix} 0 & 1 \\ 1 & 2 \end{pmatrix}. \tag{28}$$

For the stopping distance d, we then get that

$$d = \sum_{k=0}^{\infty} (A^k V, BA^k V) = (V, \sum_{k=0}^{\infty} (A^k)^t BA^k V), \tag{29}$$

where the upper script t denotes the transpose matrix. Using (26) and (28) we find that

$$(A^k)^t BA^k = 2\kappa \begin{pmatrix} 0 & (e_t e_n)^k \\ (e_t e_n)^k & 2e_n^{2k} + 4\sum_{i=1}^{k} e_t^i e_n^{2k-i} \end{pmatrix}. \tag{30}$$

Now inserting (30) into (29) then yields

$$d = 4\kappa \left[uv \sum_{k=0}^{\infty} (e_t e_n)^k + v^2 \sum_{k=0}^{\infty} e_n^{2k} + 2v^2 \sum_{k=0}^{\infty} \sum_{i=1}^{k} e_t^i e_n^{2k-i} \right]. \tag{31}$$

The first two sums above are geometrical series, $\sum_{k=0}^{\infty}(e_t e_n)^k = 1/(1 - e_t e_n)$ and $\sum_{k=0}^{\infty} e_n^{2k} = 1/(1 - e_n^2)$, while the double sum gives

$$\sum_{k=0}^{\infty} \sum_{i=1}^{k} e_t^i e_n^{2k-i} = \frac{e_t e_n}{(1 - e_n^2)(1 - e_t e_n)}\,. \tag{32}$$

Substituting these expressions into (31) and performing some simplification, one arrives at formula (20). □

We can now state and prove the following result concerning the existence of nontrivial halting orbits.

Theorem 3 *The map F given in (10) and (11) has non-trivial halting orbits if and only if $\kappa \leq \kappa_s$, where*

$$\kappa_s \equiv \frac{(1 - e_t e_n)(1 - e_n^2)}{1 + 3e_n(e_t + e_n) + e_t e_n^3}. \tag{33}$$

Proof. Let the particle fall off the edge of a step with zero initial velocity. The particle then hits the next step at $z' = 1 - \kappa$ and just after bouncing has velocity $V = (e_t, e_n)$, as can be checked from (11). The stopping distance d_0 for this case can be evaluated from the previous Lemma:

$$d_0 = \frac{4\kappa(e_n + e_t)e_n}{(1 - e_t e_n)(1 - e_n^2)}. \tag{34}$$

The particle comes to a stop before it reaches the edge of the ramp provided that $d_0 \leq 1 - \kappa$, which means $\kappa < \kappa_s$. This proves the 'if' part. Next note that whenever a particle lands on a ramp, the value for u must be greater than e_t and the value for v must be greater than e_t (just after landing). Thus we have that d is greater than d_0. Since also z at the landing point must be smaller than $1 - \kappa$, we see that if $\kappa > \kappa_s$ then $d > 1 - \kappa$ and the particle cannot come to a stop. □

One can easily verify that $0 < \kappa_\infty < \kappa_s < 1$. Thus for $\kappa_\infty < \kappa \leq \kappa_s$ both unbounded and halting orbits coexist. In fact, we will see in Sec. 6 below

that in this case there exist other types of bounded orbits, namely, periodic orbits. We conjecture that for $\kappa > \kappa_s$, where no halting orbits exist, all orbits are unbounded, whereas for $\kappa < \kappa_\infty$, where no unbounded orbit is possible, all orbits are halting ones. (These conjectures are supported by our numerics where a bounded orbit was never found for $\kappa > \kappa_s$ nor a non-halting orbit was ever found for $\kappa < \kappa_\infty$.)

5 Fixed Points

When we try to solve for the fixed points of the map (11) by setting $u' = u$, $v' = v$, and $z' = z$, we immediately encounter a curious fact, namely, that the variable z immediately drops out of its fixed-point equation. As we will see below, this implies that for given e_t and e_n fixed points will exist only for a specific value of the parameter κ.

Let us suppose that there exists a fixed point where the particle jumps m steps every iterate. Then setting $n = m$, $u' = u = u^*_m$ and $v' = v = v^*_m$ in (11) and solving for the fixed-point value of velocity components u^*_m and v^*_m, one readily obtains

$$u^*_m = \frac{e_t}{1 - e_t}\sqrt{\frac{m(1 + e_n)}{1 - e_n}}, \tag{35}$$

$$v^*_m = e_n\sqrt{\frac{m}{1 - e_n^2}}. \tag{36}$$

Now consider the equation for z'. Setting $n = m$ and $u' = u = u^*_m$ in (12) and performing some simplification yield

$$z' = z + m\left(1 - \frac{\kappa}{\kappa_\infty}\right), \tag{37}$$

where κ_∞ is as given in (15). From (37) it immediately follows that fixed points (i.e., $z' = z$) can exist only if $\kappa = \kappa_\infty$. It is also clear that the above fixed points will exist if and only if there are values of $z \in [0, 1)$ such that the condition (14) is satisfied for $\kappa = \kappa_\infty$, $u = u^*_m$, $v = v^*_m$, and $n = m$. The following calculation establishes that this indeed occurs.

Setting $\kappa = \kappa_\infty$, $u = u^*_m$, $v = v^*_m$, and $n = m$ in (14), we obtain after some simplification:

$$2\sqrt{m} \geq (1-e_n)\sqrt{m} + (1+e_n)\left[m - 2\frac{(1+e_t)(1-e_n)}{e_t+e_n}z\right]^{1/2} > \\ > 2\sqrt{m-1+e_n^2}. \tag{38}$$

It is easy to see that the first inequality implies that $z \geq 0$, while the second inequality yields $z < z_m$, where

$$z_m = \frac{2(e_t+e_n)}{(1+e_t)(1+e_n)^2}\left[1+e_n-m+\sqrt{m(m-1+e_n^2)}\right]. \tag{39}$$

[Note that z_m is an increasing function of m and that $\lim_{m\to\infty} z_m = \frac{1}{2}(1-\kappa_\infty)$.] Thus, for each $m > 0$ there exists an interval I_m

$$I_m \equiv [0, z_m), \tag{40}$$

such that for $z \in I_m$ the condition (14) holds. We have thus established the following result.

Proposition 4 *For every integer $m > 0$, the map F given in (10) and (11) has a segment $C_m \equiv \{(u_m^*, v_m^*, z) \mid z \in I_m\}$ of fixed points with jump number m if and only if $\kappa = \kappa_\infty$.*

Next we turn to discuss the stability of the fixed points. Let us denote by DF the Jacobian matrix of the map (11). Calculating DF and performing some simplification, one finds that DF can be written in the following form

$$DF = \begin{pmatrix} e_t & e_n(u'-e_tu)/v' & 0 \\ 0 & e_n^2 v/v' & 0 \\ -2\kappa(u'/e_t - u) & -2\kappa u'(u'-e_tu)/e_t^2 v' & 1 \end{pmatrix}. \tag{41}$$

Setting $\kappa = \kappa_\infty$, $n = m$, $u' = u = u_m^*$, and $v' = v = v_m^*$ into (41), we readily find that the Jacobian matrix at the fixed point becomes

$$DF|_{\text{f.p.}} = \begin{pmatrix} e_t & e_t(1+e_n) & 0 \\ 0 & e_n^2 & 0 \\ -2\frac{(1-e_t)}{(1+e_t)}\sqrt{\frac{(1-e_n)m}{(1+e_n)}} & -2\frac{\sqrt{(1-e_n^2)m}}{1+e_t} & 1 \end{pmatrix} \tag{42}$$

It is easy to see that the eigenvalues of this matrix are given by the diagonal entries: $\lambda_1 = e_t$, $\lambda_2 = e_n^2$, and $\lambda_3 = 1$. Although the first two eigenvalues (associated with the equations for u' and v', respectively) are positive and

smaller than 1, the third eigenvalue (from the equation for z') is equal to unity, so that the fixed points are marginally stable. This property is clearly a consequence of the translational invariance in the z coordinate of the fixed points. Because of this fact, the question of stability of the fixed points must be considered with some caution.

Small perturbations in the velocity from the fixed point will decrease exponentially fast because the relevant eigenvalues λ_1 and λ_2 are both smaller than 1. However, before the velocity converges to the fixed point (u_m^*, v_m^*) the value of z might become outside the interval J_m, thus leading to a change in jump number. One can show that this cannot happen if we pick an initial velocity sufficiently close to the fixed point and a value of z sufficiently far from the edge of the ramp. We thus have the following result, the formal proof of which will be published elsewhere.

Proposition 5 *The segment C_m of fixed points is an attractor for the map F in the following sense: There is an open set U_m of initial conditions such that if $x \in U_m$ then $\lim_{n\to\infty} F^n(x) \in C_m$*

It is worthwhile noting here that if one finds a periodic orbit, then the previous result will also hold for that periodic orbit. The most important observation needed to establish this is that equation (41) implies that the eigenvalues of the derivative along a q-periodic orbit can easily be calculated. Suppose $x = (u, v, z)$ is a point belonging to a q-periodic orbit of F. Then one can easily check that the derivative DF^q of F^q evaluated at x is of the form

$$DF = \begin{pmatrix} e_t^q & * & 0 \\ 0 & e_n^{2q} & 0 \\ * & * & 1 \end{pmatrix}.$$

Here $*$ stands for an arbitrary entry. For the same reasons as before the eigenvalues of this matrix are e_t^q, e_n^{2q} and 1. Thus the contraction rates along the invariant manifolds of a periodic orbit are the same as those for the fixed points, and hence the periodic orbits will be stable in the sense described in Proposition 5. In the next section we will consider several periodic orbits for which explicit solutions can be found.

6 Periodic Orbits

Here we consider two classes of periodic of orbits: i) orbits of arbitrary period $k+1$, with $k = 1, 2, ...$, where the particle jumps k times with $n = 0$ and then

once with $n = 1$; and ii) orbits of period 2 where the particle jumps m steps once and then $m + 1$ steps in the next flight. For convenience of notation we shall label the periodic orbits by juxtaposing the corresponding jump number for each point of the orbit. For instance, orbits of class i) above will be labelled by 000...01 (meaning k zeros followed by 1). More compactly, we shall refer to these orbits as being orbits of type 0^k1. Similarly, the periodic orbits in class ii) will be said to be of type $m(m + 1)$.

6.1 Periodic orbits of type 0^k1

In order to obtain an explicit solution for periodic orbits of type 0^k1 a somewhat tedious calculation is required, and here we give only its main steps. Since in this case the particle bounces k times with $n = 0$, we can use the results of Sec. 4: if $V = (u, v)^t$ denotes the vector velocity at the beginning of the first flight, then the velocity $V_k = (u_k, v_k)^t$ after the next k collisions will be given by $V_k = A^k V$, where A^k is as in (26). Upon performing the sum in (26) one finds

$$u_k = e_t^k u + \frac{2e_t(e_n^k - e_t^k)}{e_n - e_t} v, \tag{43}$$

$$v_k = e_n^k v. \tag{44}$$

Similarly, the distance d_k traversed after these k flights can be obtained from the same reasoning that lead to formula (31):

$$d_k = 4\kappa \left[uv \sum_{j=0}^{k-1} (e_t e_n)^j + v^2 \sum_{j=0}^{k-1} e_n^{2j} + 2v^2 \sum_{j=0}^{k-1} \sum_{i=1}^{j} e_t^i e_n^{2j-i} \right]. \tag{45}$$

After performing the sums above one gets

$$d_k = 4\kappa \left(\alpha_k uv + \beta_k v^2 \right), \tag{46}$$

where

$$\alpha_k = \frac{1 - (e_n e_t)^k}{1 - e_n e_t}, \quad \beta_k = \frac{(e_n + e_t)(1 - e_n^{2k})}{(e_n - e_t)(1 - e_n^2)} - \frac{2e_t(1 - e_n^k e_t^k)}{(e_n - e_t)(1 - e_n e_t)}. \tag{47}$$

If we denote by z the particle position at the beginning of the first flight, then the position after k flights is simply

$$z_k = z - d_k. \tag{48}$$

The particle now jumps once with $n = 1$, so that according to (11) the velocity (u_{k+1}, v_{k+1}) at the beginning of next flight is given by

$$u_{k+1} = e_t \left(u_k + v_k + \sqrt{v_k^2 + 1} \right), \tag{49}$$

$$v_{k+1} = e_n \sqrt{v_k^2 + 1}. \tag{50}$$

One then has to solve the fixed-point equations, namely, $u_{k+1} = u = u_0$ and $v_{k+1} = v = v_0$. Here we omit the details and simply quote the final result

$$u_0 = \frac{e_n - e_t + (e_n + e_t)e_n^{k+1} - 2e_n e_t^{k+1}}{(e_n - e_t)(1 - e_t^{k+1})} \frac{e_t}{\sqrt{1 - e_n^{2(k+1)}}}, \tag{51}$$

$$v_0 = \frac{e_n}{\sqrt{1 - e_n^{2(k+1)}}}. \tag{52}$$

Now consider the equation for the particle position z_{k+1}. From (12) one has

$$z_{k+1} = z_k + 1 - \kappa \left(\frac{u_{k+1}^2}{e_t^2} - u_k^2 \right). \tag{53}$$

Setting $u_{k+1} = u = u_0$ in this equation and using (43), (46), and (48), one can show after some algebra that z_{k+1} can be written in the following form

$$z_{k+1} = z + 1 - \frac{\kappa}{\kappa_{0^k 1}}, \tag{54}$$

where

$$\kappa_{0^k 1} = \frac{1}{4} \left[a_k u_0^2 + b_k u_0 v_0 + c_k v_0^2 \right]^{-1}. \tag{55}$$

Here u_0 and v_0 are as in (51) and (52), and the constants a_k, b_k and c_k are given by

$$a_k = \frac{1 - e_t^{2(k+1)}}{4e_t^2}, \; b_k = \alpha_k - \frac{e_t^{k+1}(e_n^k - e_t^k)}{e_n - e_t}, \; c_k = \beta_k - \left[\frac{e_t(e_n^k - e_t^k)}{e_n - e_t} \right]^2. \tag{56}$$

We thus see from (54) that, just as in the case of fixed points, periodic orbits of type $0^k 1$ can exist only at specific values of κ, namely, for $\kappa = \kappa_{0^k 1}$. In order to show that these periodic orbits do indeed exist we need to verify that there are values of z such that condition (13) is satisfied at $\kappa = \kappa_{0^k 1}$ for $u = u_0$ and $v = v_0$. This condition immediately yields a minimum value for z:

$z \geq z^k_{\min} \equiv 4\kappa_{0^k1} v_0(u_0+v_0)$. Now note that we must have $z_k < 4\kappa_{0^k1} v_k(u_k+v_k)$ since the $(k+1)$th flight has $n=1$. In view of (48) this last inequality implies $z < z^k_{\max} \equiv d_k + 4\kappa_{0^k1} v_k(u_k+v_k)$. One can also verify that $0 < z^k_{\min} < z^k_{\max} < 1$. Thus for z in the interval $J_k \equiv [z^k_{\min}, z^k_{\max})$ the condition (13) will be satisfied and the periodic orbits do exist. We have thus proven the following result.

Proposition 6 *For every integer $k > 0$, the map F given in (10) and (11) has periodic orbits of type 0^k1 if and only if $\kappa = \kappa_{0^k1}$. Moreover, the first point with $n = 0$ in these orbits can be arbitrarily chosen from the segment $C_k \equiv \{(u_0, v_0, z) \mid z \in J_k\}$, with u_0 and v_0 being given by (51) and (52), respectively.*

One can verify that $\kappa_{0^k1} < \kappa_{0^l1}$ for $k < l$ and that $\lim_{k\to\infty} \kappa_{0^k1} = \kappa_s$. We thus have the seemingly counterintuitive fact 'slower orbits' occur for larger inclinations. We also remark that the procedure above could, in principle, be extended to other classes of periodic orbits, for example, orbits of type 0^k10^l1. (The calculation, of course, becomes exceedingly complicated and will not be attempted here.) In fact, we conjecture that to each sequence in $\{0,1\}^{\mathbb{N}}$ compatible with rotations on the circle by a rational angle, we can associate an orbit whose jump numbers form that sequence. Periodic orbits with jump numbers other 0 and 1 also exist as we show next.

6.2 Periodic orbits of type $m(m+1)$

Now we consider a periodic orbit of period 2 with jump numbers $n_1 = m$ and $n_2 = m+1$. Here we only need to consider the case $m > 0$, since $m = 0$ corresponds to the orbit 01 which belongs to the class of orbits studied above. Let us denote the two points of the periodic orbit by $x_1 = (u_1, v_1, z_1)$ and $x_2 = (u_2, v_2, z_2)$, respectively, where $F(x_1) = x_2$ and $F(x_2) = x_1$. In order to find such an orbit let us iterate the map (11) twice, first with $n = m$ and then with $n = m+1$. For the second iterates of u and v we respectively find

$$u'' = e_t\left[e_t(u+v) + (e_t+e_n)\sqrt{v^2+m} + \sqrt{e_n^2v^2 + m(1+e_n^2)+1}\right], \qquad (57)$$

$$v'' = e_n\sqrt{e_n^2v^2 + m(1+e_n^2)+1}. \qquad (58)$$

We now solve for the fixed points of these equations. First note that the second equation above can be written as a linear equation in v^2, and so it has a unique positive solution:

$$v_1 = e_n\sqrt{\frac{1+m(1+e_n^2)}{1-e_n^4}}\quad , \qquad (59)$$

which upon substitution back into (58) gives

$$v_2 = e_n \sqrt{\frac{e_n^2 + m(1+e_n^2)}{1-e_n^4}} \quad . \tag{60}$$

Performing a similar calculation for the fixed point of (57), one then finds the following values:

$$u_1 = \frac{e_t}{e_n(1-e_t^2)} \left[(1+e_t e_n)v_1 + (e_t+e_n)v_2\right] \quad , \tag{61}$$

$$u_2 = \frac{e_t}{e_n(1-e_t^2)} \left[(e_t+e_n)v_1 + (1+e_t e_n)v_2\right] \quad , \tag{62}$$

with v_1 and v_2 as given in (59) and (60), respectively.

Let us now consider the second iterate of the variable z. Using (12) it can be readily verified that z'' can be written as

$$z'' = z + 2m + 1 - \kappa e_t^{-2} \left[u''^2 + (1-e_t^2)u'^2 - e_t^2 u^2\right], \tag{63}$$

which for $u'' = u = u_1$ and $u' = u_2$ becomes

$$z'' = z + 2m + 1 - \kappa(e_t^{-2} - 1)\left(u_1^2 + u_2^2\right). \tag{64}$$

Inserting (61) and (62) into (64) and performing some simplification, one finds

$$z'' = z + (2m+1)\left[1 - \frac{\kappa}{\kappa_{m(m+1)}}\right], \tag{65}$$

where

$$\kappa_{m(m+1)} = \left[\frac{4e_t e_n + (1+e_t^2)(1+e_n^2)}{(1-e_t^2)(1-e_n^2)} \quad + \right.$$
$$\left. + \quad \frac{4(e_t+e_n)(1+e_t e_n)}{(1-e_t^2)(1-e_n^4)} \frac{\sqrt{e_n^2 + (1+e_n^2)^2 m(m+1)}}{(2m+1)}\right]^{-1} . \tag{66}$$

Note that $\kappa_{m(m+1)} > \kappa_{m'(m'+1)}$ for $m < m'$ and that $\lim_{m\to\infty} \kappa_{m(m+1)} = \kappa_\infty$, with κ_∞ as given in (15). [One can also verify that for $m = 0$ the expression above for κ_{01} yields the same value as obtained by setting $k = 1$ in (55).]

From (65) it is clear that periodic orbits of period 2 (i.e., $z'' = z$) can exist only if $\kappa = \kappa_{m(m+1)}$. As before, in order to ensure that these periodic orbits

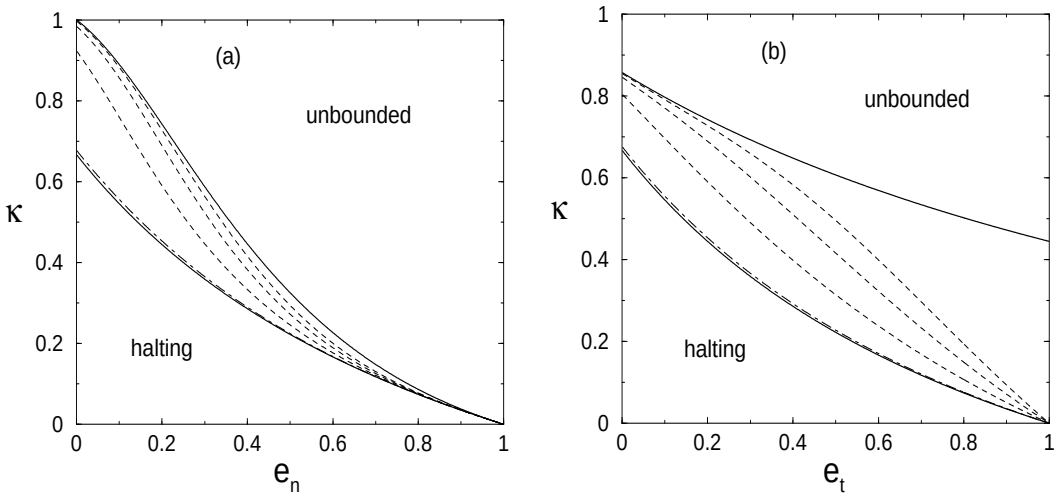

Fig. 2. Phase diagram for the map F: (a) in the plane $e_t = 0.2$ and (b) in the plane $e_n = 0.2$. The lower and upper solid curves represent κ_∞ and κ_s, respectively; the three dashed lines give κ_{01}, κ_{001} and κ_{0001} (from the bottom up); whereas the dot-dashed line corresponds to κ_{12}.

do indeed exist we need to verify that the condition (14) holds at $\kappa = \kappa_{m(m+1)}$ for $n = m$, $u = u_1$, $v = v_1$ and for some $0 \leq z < 1$. (Recall that we only need to check for $m > 0$.) Such calculation is similar to that performed earlier for the case of the fixed points, only much more awkward and so it will not be presented here. The result is that there will be an interval $J_m \subset [0, 1)$ such that for $z \in J_m$ the condition (14) holds. We thus have

Proposition 7 *For every $m \geq 0$, the map F has periodic orbits of period 2 with jump numbers $n_1 = m$ and $n_2 = m + 1$ if and only if $\kappa = \kappa_{m(m+1)}$. Moreover the velocities (u_1, v_1) and (u_2, v_2) are uniquely given by (59)–(62).*

7 Discussion and Conclusions

The analysis presented above can be summarized in the 'phase diagram' shown in Fig. 2, which we now proceed to discuss. In this figure the lowermost and uppermost curves represent, respectively, the surfaces $\kappa_\infty(e_n, e_t)$ and $\kappa_s(e_n, e_t)$ cut at the planes $e_t = 0.2$ (Fig. 2a) and $e_n = 0.2$ (Fig. 2b). These two surfaces separate the parameter space (e_n, e_t, κ) into three distinct regions. We conjecture (and have verified numerically) that in the region $\kappa > \kappa_s(e_n, e_t)$, where no halting orbits exist, only unbounded orbits can occur, whereas in the region $\kappa < \kappa_\infty(e_n, e_t)$, where no unbounded orbit is possible, only halting orbits occur. In the middle region, $\kappa_\infty(e_n, e_t) < \kappa < \kappa_s(e_n, e_t)$, not only halting and unbounded orbits coexist but there are also periodic orbits of arbitrary period. Shown in Fig. 2 as dashed lines are the corresponding surfaces κ_{01},

κ_{001}, and κ_{0001} at which periodic orbits of types 01, 001, and 0001 exist. Also shown as a dot-dashed line is the surface κ_{12} at which a periodic orbit of type 12 appears. We have argued above that many other periodic orbits should exist for $\kappa_\infty(e_n, e_t) < \kappa < \kappa_s(e_n, e_t)$. In fact we conjecture that periodic orbits are dense in this region.

It is interesting to compare the conclusions above with what was found in our earlier model [10], where $e_n = 0$ and the particle was allowed to slide frictionlessly. We shall refer to this previous model as *model 1*, while the model discussed in the present paper will be called *model 2*. Model 1 was considerably simpler to analyze since its dynamics is described by a one-dimensional map [10]. Its phase diagram contains a curve $\kappa_\infty(e_t)$ such that if $\kappa < \kappa_\infty(e_t)$ then all orbits are bounded, whereas if $\kappa > \kappa_\infty(e_t)$ all orbits are unbounded. In this sense, the transition between bounded and unbounded motion is 'sharp' in model 1. Comparing the phase diagram of the two models, we thus see that it is as if the curve $\kappa_\infty(e_t)$ of model 1 has 'opened up' in model 2 into a region, namely, $\kappa_\infty(e_t, e_n) < \kappa < \kappa_s(e_n, e_t)$, where one now has coexistence of halting, unbounded and periodic orbits.

In a separate paper [13] we have combined these two models by allowing the particle to slide, on the account of gravity, after it has come to a halt. In this case, upon sliding until the end of the step the particle then embarks on a ballistic flight, at which point we resume iteration of the bouncing map F. Preliminary results on this hybrid model were given in Ref. [13] and a more detailed analysis of its dynamics will be the subject of a forthcoming publication [14]. Here however we wish emphasize, as a concluding remark, that no matter how one chooses to restart the motion after the particle comes to a halt, the particle velocity remains always bounded in the region $\kappa < \kappa_\infty(e_t, e_n)$.

This work was supported in part by FINEP, CNPq, and PRONEX under grant number 76.97.1004.00.

A Appendix

Here we show that the quantity γ defined in (16) becomes vanishingly small as the velocity (u, v) becomes arbitrarily large. First we note that γ can be rewritten as

$$\gamma = \sqrt{v^2 + n} - \left[\frac{\kappa(u+v)}{1-\kappa} + \frac{\sqrt{(\kappa u + v)^2}}{1-\kappa} \right].$$

In what follows we will use the fact that

$$|\sqrt{x} - \sqrt{x-1}| \leq \frac{1}{\sqrt{x}}\,, \quad \forall x \geq 1,$$

and that $0 \leq z < 1-\kappa$. (This last relation follows from the fact that the largest z is obtained when the particle falls off the edge of a step with zero initial velocity.) If $n \geq 1$, the condition (14) together with the inequalities just mentioned imply that

$$0 \leq \sqrt{v^2+n} - \left(\frac{\kappa(u+v)}{1-\kappa} + \frac{[(\kappa u+v)^2 - z(1-\kappa)]^{1/2}}{1-\kappa} \right) =$$

$$\gamma + \left[\frac{[(\kappa u+v)^2}{(1-\kappa)^2} \right]^{1/2} - \left[\frac{(\kappa u+v)^2}{(1-\kappa)^2} - \frac{z}{(1-\kappa)} \right]^{1/2} \leq \gamma + \frac{1-\kappa}{\kappa u+v}\,.$$

Furthermore, again by equation (14) we have

$$\frac{1}{\sqrt{v^2+n}} \geq \sqrt{v^2+n} - \sqrt{v^2+n-1} >$$

$$\sqrt{v^2+n} - \left(\frac{\kappa(u+v)}{1-\kappa} + \frac{[(\kappa u+v)^2 - z(1-\kappa)]^{1/2}}{1-\kappa} \right) > \gamma\,.$$

Putting these equations together, we obtain that γ is inversely proportional to the velocity in the following sense

$$-\frac{1-\kappa}{\kappa u+v} \leq \gamma < \frac{1}{\sqrt{v^2+n}}\,.$$

References

[1] J. Rajchenbach, Phys. Rev. Lett. 65 (1990) 2221.

[2] P.-A. Lemieux, D. J. Durian, Phys. Rev. Lett. 85 (2000) 4273.

[3] D. J. Durian, J. Phys.: Condens. Matter 12 (2000) A507.

[4] L. Samson, I. Ippolito, D. Bideau, G. G. Batrouni, Chaos 9 (1999) 639; and references therein.

[5] C. Ancey, P. Evesque, P. Coussot, J. Phys. I 4 (1994) 1161.

[6] G. G. Batrouni, S. Dippel, L. Samson, Phys. Rev. E 53 (1996) 6496.

[7] S. Dippel, G. G. Batrouni, D. E. Wolf, Phys. Rev. E 54 (1996) 6845; *ibid.* 56 (1997) 3645.

[8] A. Valance, D. Bideau, Phys. Rev. E 57 (1998) 1886.

[9] U. M. B. Marconi, M. Conti, A. Vulpiani, Europhys. Lett. 51 (2000) 685.

[10] G. L. Vasconcelos, J. J. P. Veerman, Phys. Rev. E 59 (1999) 5641.

[11] G. L. Vasconcelos, J. J. P. Veerman, Physica A 271 (1999) 251.

[12] S. F. Foerster, M. Y. Lounge, H. Chang, K. Allia, Phys. Fluids 6 (1994) 1108.

[13] G. L. Vasconcelos, F.V. Cunha-Jr., J. J. P. Veerman, Physica A 295 (2001) 261.

[14] F.V. Cunha, Jr., G. L. Vasconcelos, J. J. P. Veerman, in preparation.